The following manuscript is the preprint version of the paper that has been published in Electrochimica Acta, vol. 223, p. 71-77, April 2017.
The final version can be found here: https://authors.elsevier.com/a/1Uhpn33-e9ceh

doi:10.1016/j.electacta.2017.03.012

Optimal Surface Doping of Lead for Increased Electrochemical Insertion of Hydrogen into Palladium

Steven C. Hamm, David L. Knies, Olga Dmitriyeva, Richard Cantwell, Matt McConnell*

Coolescence LLC, 2450 Central Avenue Suite F, Boulder, Colorado 80301, United States

ABSTRACT

Increasing the amount of hydrogen that is electrochemically inserted into materials is important for studying superconductivity and hydrogen embrittlement, and improving hydrogen storage capabilities. Surfaces can be engineered to accomplish this task with better insight into how the composition of a material's first few atomic layers affects the electrochemical insertion of hydrogen. To this end, between 1 μg cm^{-2} and 23 μg cm^{-2} of Pb was deposited onto Pd cathodes during galvanostatic experiments in the 0.1 M LiOH electrolyte. The optimum surface doping level 2.9 μg cm^{-2} of Pb (~1.4 mass equivalent monolayers) was found to achieve the highest quantity of inserted hydrogen at approximately −0.5 V vs RHE. Additionally, the hydrogen content increased

from $PdH_{0.75}$ to $PdH_{0.86}$ with increasing Pb amounts up to 2.9 μg cm^{-2} at a constant current of −14.5 mA cm^{-2}. For comparison, the same change in hydrogen content from pressurized gas loading experiments would require an increase in hydrogen fugacity from about 6 to 1420 atm. Preliminary analysis concerning the adsorbed hydrogen chemical potential suggests the Pb is affecting the balance between the Volmer, Heyrovsky, and Tafel reaction rates, which changes the hydrogen surface chemical potential, and ultimately controls the hydrogen insertion. Furthermore, the addition of Pb was found to decrease the rate of hydrogen insertion. This work provides a fundamental basis for the future design of metal surfaces yielding enhanced electrochemical hydrogen insertion in Pd and other hydrogen absorbing materials.

KEYWORDS: Palladium hydride, hydrogen storage, hydrogen insertion, promoter, lead

1. INTRODUCTION

Electrochemical insertion of hydrogen in materials is of interest for superconductivity studies [1], hydrogen embrittlement studies [2], and hydrogen storage applications [3,4]. Modifying the surface of metals with known hydrogen insertion promoters (e.g. Pb, As, thiourea, *etc.*) can increase the adsorbed hydrogen chemical potential obtained during aqueous electrolysis [5,6]. Diffusion of the hydrogen into the bulk ensues due to the chemical potential gradient, resulting in an elevated hydrogen content in the bulk of the electrode material. Quantities as small as nanomolar of insertion promoters in the electrolyte have resulted in such effects [5]. Hydrogen insertion promoters are commonly used to study hydrogen embrittlement [2], and has also garnered interest in enhancing the hydrogen storage capability of materials [3,7]. Although a number of explanations for the insertion enhancement obtained by non-metallic insertion promoters (e.g.

thiourea [3,8,9], As [10], H_2S [11]) have been presented, explanations as to how the addition of surface metals behave as insertion promoters is still lacking.

A better understanding of how the addition of surface metals affect hydrogen insertion could lead to the engineering of surfaces to maximize such an effect. Pd was chosen as the cathode material to study the effects of the surface promoter Pb on hydrogen insertion. Pd is a material known to absorb large quantities of hydrogen, reaching $PdH_{0.69}$ at 1 atm H_2 [12]. The hydrogen content in palladium hydrides can be simply determined by the measurement of electrical resistance as there is a well-studied relationship between electrical resistance and hydrogen content up to $PdH_{1.0}$ [12–14]. Galvanostatic measurements were performed to observe the changes in electrode potential and hydrogen content under different effective Pb surface coverages. The results show that there is an optimum Pb coverage ~ 3 μg cm^{-2} to achieve the maximum hydrogen content at ~ −0.5 V vs RHE. At this coverage, the reaction route is likely a mixture between Volmer-Tafel (V-T) and Volmer-Heyrovsky (V-H) routes. The Pb is likely acting to suppress the Tafel reaction, making it possible to get a higher chemical potential for hydrogen on the surface without fully enabling the Heyrovsky mechanism. Above this coverage, the reaction route begins to change to primarily V-H. This finding suggests that surfaces can be engineered to maximize hydrogen insertion under given working conditions.

2. EXPERIMENTAL SECTION

2.1. Cathode Assembly for Simultaneous Resistance Measurements.

The Pd cathode was placed in a configuration to allow four-point resistance measurements simultaneously with the electrochemical experiments. An illustration of the cathode assembly can be found in Fig. S1(a) in the supplementary material. Pd cathodes were fabricated in-house by cold

rolling sections of a Pd sputter target (ESPI, 99.95%) to a thickness of 40-50 μm. The final passes through the mill were made with polished rollers to produce a mirror finish on the cathodes. The Pd cathodes were cut to dimensions of 7 mm × 40 mm. Two 4.1 mm diameter holes were punched in the ends of the foils so that polyether ether ketone (PEEK) screws could thread through to immobilize the cathode and provide mechanical compression for the electrical connections with 50 μm thick Pt flags. One of the Pt flags was 10 mm × 10 mm and had two Pt wires for four-point resistance measurements and one Pt wire for power. Another Pt flag was 10 mm × 7.5 mm and had the other two Pt wires for four-point resistance measurements. All Pt wires were spot-welded to the Pt flags using high-melting point tungsten welding tips to reduce the possibility of contamination. The Pt flags also had 4.1 mm diameter holes punched out. The cathode was placed on a polytetrafluoroethylene (PTFE) support between two PEEK spacer blocks, followed by the Pt foils, the Pd cathode, and another PEEK spacer block. The assembly was fastened to the PTFE support with PEEK screws and nuts. As assembled, the total exposed Pd (including front and back geometric areas) in contact with electrolyte was 2.8 cm^2. All Pt wires were encapsulated with PTFE/FEP dual shrink tubing (Zeus) and the PEEK blocks were sized to minimize the effect of Pt on the electrochemical measurements.

2.2. Cathode Cleaning.

The Pd foils and cathode assembly were cleaned of impurities so that only the effects of Pd and Pb were observed. The as-rolled and sized Pd foils were first cleaned by sonicating at room temperature in isopropyl alcohol (IPA) followed by sonication in acetone for 5 min each. The foils were then rinsed in IPA and DI water. The foils were placed in a vial that contained concentrated HNO_3 (trace metal grade, Fisher Chemical) and kept at a 90 °C for 40 min. Finally, the foils were

rinsed in DI water and blow dried by compressed difluoroethane gas (Falcon Dust-Off). The cathode was then placed in the assembly which was subsequently soaked in 5% HNO_3 and rinsed in DI water prior to placing into the electrolyte. The cell preparation and experiments were performed under a NuAire horizontal laminar flow hood (NU-301-630) to prevent environmental contamination.

2.3. Configuration of Electrochemical Cell.

A borosilicate glass split-cell was used to prevent the deposition of Pt on the cathode and remove the effects of O_2 on the electrochemical experiments. An illustration of the cell can be found in Fig. S1(b) in the supplementary material. The cell had a water jacket to maintain the cell at 25 °C via a water chiller. The two sides of the cell were separated by a Nafion™ 1110 proton exchange membrane. A batch of membranes were cleaned by soaking in 5% HNO_3 at 60 °C for at least two hours, and subsequently stored in a fresh 5% HNO_3 solution at room temperature until use. A new membrane was used for each experiment after rinsing in DI water. The electrolyte on the cathode side of the cell was 0.1 M LiOH, which was prepared in-house in a glove bag under an Ar environment by dissolving Li metal (Sigma-Aldrich, ribbons or granular > 99% trace metals basis) in DI water. A reversible hydrogen electrode (RHE; Gaskatel Hydroflex® RHE) was also placed in the 0.1 M LiOH compartment. The electrolyte on the anode side of the cell was 0.1 M H_2SO_4 (Fisher Scientific, trace metal grade). Fresh electrolytes were prepared for every experiment. The anode for all experiments was a Pt foil of dimension 10 mm × 40 mm, also with two holes punched, and a spot-welded Pt wire lead. Heavy Ar purging (>100 bubble s^{-1}) was performed for at least 10 min prior to starting all experiments and slow Ar bubbling (1-2 bubble s^{-1}) was maintained on both sides of the cell throughout the experiments to purge of O_2 and CO_2 in the

cathode compartment. A thermocouple for cell temperature measurements was placed in the solution through a PTFE sleeve which was pinned near the bottom of the cathode. The cell was thermally stabilized for at least 10 min before running the experiments.

2.4. Pb Doping Solution.

Pb was deposited on the cathode by adding a solution containing Pb directly into the electrolyte during electrolysis. The Pb doping solution was prepared by dissolving Pb in 0.1 M LiOH in a water bath at 90 °C for 4.5 h. The Pb concentration was measured by inductively coupled plasma mass spectroscopy (ICP-MS). This solution was then diluted to a concentration of 10 ppm Pb in 0.1 M LiOH. The amount of Pb added to the electrolyte is reported as μg per cathode geometric area (i.e. μg cm^{-2}). It is assumed that the cathode-to-cathode difference in electrochemical surface area is small, considering they were all prepared the same way. The Ar flow was increased to >100 bubbles s^{-1} for about 10-15 min after doping the electrolyte to mix the solution.

2.5. Electrochemical Measurement Procedure.

The electrochemical measurement protocol was designed to provide the necessary data to observe changes in hydrogen insertion as a function of current density (j), and calculate the Tafel slopes and exchange current densities obtained from Tafel plots. Electrochemical measurements were performed using a Bio-Logic potentiostat/ galvanostat module. All applied current densities throughout the experiment were cathodic and are reported here with respect to the Pd geometric surface area of 2.8 cm^2. A constant current of −3.6 mA cm^{-2} was applied to the Pd electrode for about 15.5 h to reach a steady state hydrogen content. Afterward, the electrolyte was spiked with Pb without disrupting the current, which was maintained for another 4 h. Next, galvanostatic

stepping was performed from -0.18 mA cm^{-2} to -18 mA cm^{-2} in -1.8 mA cm^{-2} increments holding for about 1 h at each current density. The first iteration of the stepping protocol will be referred to as galvanostatic step (GS) cycle 1. Subsequently, the cathode was held at -3.6 mA cm^{-2} again for about 4 h and the stepping protocol was repeated (referred to as GS cycle 2, and so on). Fig. S2 in the supplementary material shows the protocol in detail. All the data presented in this work was obtained from GS cycle 2 so that adequate time was allowed for Pb deposition. The hydrogen content reported herein was obtained at the end of each galvanostatic step when the hydrogen content was near a steady state value.

The cathode potential at the end of each galvanostatic step was corrected for the ohmic drop across the 0.1 M LiOH electrolyte resistance, R_{el}. The electrolyte resistance was obtained at the end of each galvanostatic step using a galvanostatic electrochemical impedance spectroscopy (GEIS) measurement performed with 1 mA amplitude and a frequency of 31 kHz. The ohmic drop was found by multiplying the applied current (I) and R_{el}. Finally, overpotential, η, was taken as the difference between the measured cathode potential (E(vs RHE)) and the ohmic drop (i.e. $\eta = E(\text{vs } RHE) - IR_{el}$).

2.6. Procedure to Determine H Content.

The four-point resistance measurement was used to infer the hydrogen content in PdH_x. This technique measures the resistance ratio (resistance (R) vs initial resistance (R_o)) and determines the hydrogen content by comparing it to the extensively studied resistance ratio vs hydrogen content plots. Zhang et al. [13] fit experimental resistance ratio vs x data using the fourth order polynomial equation:

$$\frac{R}{R_o} = 1 + 1.69731x - 5.34162x^2 + 13.4472x^3 - 9.87644x^4 \qquad (1)$$

where x is the atomic H/Pd ratio. The use of this calibration equation has been found to match well with the hydrogen content calculated from *in situ* synchrotron X-ray diffraction lattice parameter measurements up to $PdH_{0.97}$, which was also obtained from electrochemical insertion and used a similar resistance measurement technique as that reported here [15].

The four-point resistance measurement was performed using an HP4263B LCR meter with 1 V_{rms} and 10 kHz signal. The LCR meter was isolated from the galvanostat via a transformer circuit. It should be noted that there were no significant differences in the measured resistance values between a cathode in air and that in the electrolyte, indicating any interference from the electrolyte on the measurement is insignificant. In addition, the contribution to the overall resistance measurement from the addition of a few ML to the surface is negligible.

The applied electrochemical measurement protocol was designed to assist in the determination of x since (1) is not an injective function (Fig. S3 in the supplementary material). The combination of increasing and decreasing current steps allowed the observation of the resistance ratio versus time as the sample absorbed/desorbed hydrogen. For instance, x was less than 0.73 if the resistance ratio increased after applying larger cathodic currents, and was greater than 0.73 if the ratio decreased. Examples for both cases can be seen in Fig. S4 in the supplementary material. Additional details of the process can be found in the supplementary material.

2.7. XPS Analysis.

XPS measurements were performed using a PHI VersaProbe II to analyze the surface state of the deposited Pb after electrolysis. The samples were irradiated using a monochromatic Al Kα source at a power of 98.7 W, with a measurement spot size diameter of 100 μm, analyzer pass energy of 5.85 eV, and 0.05 eV step size.

In addition, depth profiling was performed to verify that Pb stayed near the surface and to approximate the equivalent thickness of the Pb. The standard for comparison of the samples was a Pd foil with Pb deposited by underpotential deposition (UPD) from a solution containing 0.1 M $NaClO_4$, 1.0 mM $HClO_4$, and 1.5 mM $Pb(ClO_4)_2$ at a potential of −425 mV vs Ag/AgCl for 4 min. The potential was chosen based on the position of the observed UPD peak in CV scans (Fig. S5 in the supplementary material). Potentials more negative than this resulted in bulk Pb deposition as evidenced by a significant increase in the deposited Pb amount measured by energy dispersive X-ray spectroscopy (EDS). It was assumed that the deposition resulted in one monolayer of Pb [16]. The samples were rotated during sputtering to reduce the effects of surface roughness. Adventitious carbon was removed prior to depth profiling by Ar sputtering for 2 min at 500 V, with a beam current of 500 nA rastering over an area of 3 mm × 3 mm. Subsequently, the depth profiling was performed by sputtering at a potential of 1000 V and beam current of 500 nA rastered over an area of 2 mm × 2 mm. The amount of Pb was analyzed (45.6 W, spot size diameter of 200 μm, and analyzer pass energy of 117.4 eV) every one minute during sputtering until only Pd was observed. The total amount of sputtered Pb was calculated by integrating the measured amount with respect to time. The obtained value was then normalized to the amount of Pb measured for the UPD sample to obtain an equivalent thickness in mass equivalent ML. In other words, the technique compares the mass deposited by the experiment to the mass of 1 ML. Since this technique was used to determine a mass equivalent Pb thickness, it is unaffected by the oxidation or instability in Pb position when exposed to air.

3. RESULTS AND DISCUSSION

The galvanostatic method was used to study electrochemical insertion of hydrogen in Pd. Traditionally, Tafel plots (η vs log(|j|)) consisting of multiple galvanostatic currents are used to provide information about the kinetics of the electrochemical reactions as the surface is modified (*e.g.* Fig. S6 in the supplementary material). These experiments also simultaneously investigated the hydrogen content in PdH_x *in situ*. Therefore, relationships between x ,η, and log(|j|) can be studied as a function of the amount of Pb added to the electrolyte.

3.1. Electrochemical Results.

The level of hydrogen insertion due to Pb addition has a different behavior for galvanostatic and quasi potentiostatic conditions. Fig. 1(a) shows the calculated hydrogen content (x) obtained at the end of each current step versus current density. The hydrogen content tends to have an exponential relationship with current for more negative currents than −3.6 mA cm^{-2} for Pb additions up to 8.7 μg cm^{-2}. At the Pb addition of 23 μg cm^{-2}, the loading has reached an asymptotic value of x=0.87 at more negative currents than −10 mA cm^{-2}. The cause of this plateau is due to the prominence of the Heyrovsky reaction at the η obtained for these current densities, which will be discussed in more detail later (see section Hydrogen Evolution Reaction Mechanism). The hydrogen content obtained at a selected applied current density of −14.5 mA cm^{-2} versus Pb amount is shown in Fig. 1(b). The H content increases with increasing Pb amounts up to ~3 μg cm^{-2}. Any amount of Pb greater than ~3 μg cm^{-2} does not result in any significant changes in H content at this current density.

The hydrogen content is also shown versus the average η measured at each applied current density in Fig. 1(c). The same asymptotic trend seen above is observed here, but the behavior is observed at an η of about −0.7 V. In addition, one can also discern that the maximum η increases

with increasing Pb amount. This observation can be expected since Pb is known to be a poor hydrogen evolution reaction (HER) catalyst [17]. Fig. 1(d) shows x vs the amount of Pb added to the electrolyte obtained at a selected η of about −0.5 V. Here, a rapid rise in x with Pb amount is seen, until a peak at the Pb addition amount of ~3 μg cm^{-2} is observed. The addition of larger Pb amounts results in a decrease in x at this η. To understand the cause of the circled point (sweet spot) at the peak, possible changes in the hydrogen evolution reaction (HER) routes caused by Pb need to be examined.

3.2. Deposition of Pb.

The deposition of Pb on the Pd cathode from the LiOH electrolyte is complicated. At a pH of 13, Takahiro et al. showed the dominant Pb species to be $Pb(OH)_3^-$ [18]. Such an anionic complex would be attracted to the anode. However, Pb did in fact deposit on the cathode, as shown in the following section, but it was observed that the Pb took many hours to be removed from the solution. Thus, to gain a better understanding of how the addition of Pb in the electrolyte is affecting the hydrogen insertion, it could prove beneficial to study the state of the Pb on the cathode surface.

3.3. XPS Analysis.

The deposition of metallic Pb was confirmed through XPS analysis. Fig. 2 shows the Pb 4f XPS spectra of a sample with 2.9 μg cm^{-2} Pb and the sample with Pb deposited by UPD for comparison. There are two peaks observed for both samples at 141.7 eV and 136.9 eV, indicative of the Pb $4f_{5/2}$

and Pb $4f_{7/2}$ of metallic Pb [19], respectively. There are also two peaks observed at 143.4 eV and 138.4 eV for the sample with 2.9 μg cm^{-2} Pb that are not present in the UPD Pb sample. Literature suggests these peaks to be indicative of $Pb(OH)_2$ [20]. Similar characteristics were seen in the 1 μg cm^{-2} and 8.7 μg cm^{-2} XPS spectra (Fig. S7 in the supplementary material). However, taking into consideration that Pb should be in the metallic state at the pH and potentials used in this work [21] and that metallic Pb was found on the samples, it is currently thought that the $Pb(OH)_2$ was formed during contact with the alkaline electrolyte while removing the cathode at the end of the experiment.

XPS depth profiling (Figs. S8 and S9 in the supplementary material) was used to estimate the equivalent thickness of Pb deposited on the cathodes by comparing the mass deposited during the experiment to the mass deposited by UPD. The depth profiling measurement performed on a sample with 2.9 μg cm^{-2} indicated it to be roughly 1.4 mass equivalent ML. It should be noted that since the Pb deposition occurred well negative of the Pb^{2+} Nernst potential the number of layers is referred to as mass equivalent because it is not assumed that the Pb deposited uniformly or epitaxially. Rather, this result indicates the amount of Pb found on the surface is equivalent to that needed to form 1.4 ML. Since Pb oxidizes when exposed to air, additional *in situ* analytical techniques are required to elucidate the actual structure(s) of Pb on the surface during the experiment, which is outside the scope of this work.

3.4. Hydrogen Evolution Reaction (HER) Mechanism.

Since the Pb appears to be in the metallic form, one can ascertain that the hydrogen evolution and absorption from alkaline solutions proceeds through the following four reaction steps:

$$H_2O + M + e^- \rightleftarrows MH_{surf} + OH^- \quad (2)$$

$$2MH_{surf} \rightleftarrows 2M + H_2 \quad (3)$$

$$H_2O + MH_{surf} + e^- \rightleftarrows H_2 + OH^- + M \quad (4)$$

$$MH_{surf} \rightleftarrows M_bH_{bulk} \quad (5)$$

where the reactions are Volmer (2), Tafel (3), Heyrovsky (4), and Penetration (5), respectively. *M, M_b, H_{surf},* and H_{bulk} represent the surface metal, bulk metal, adsorbed hydrogen, and absorbed hydrogen, respectively. Each of these reactions can be rewritten as a rate equation in the Arrhenius form. The effect of Pb on the exponential prefactors and the hydrogen overpotential is of interest here.

It has been demonstrated through overpotential decay transient experiments on a Pd foil that η can be separated into two components, η_1 and η_2, such that $\eta=\eta_1+\eta_2$ [22,23]. η_1 has been attributed to the overpotential due to the Volmer reaction [22], and η_2 is the hydrogen overpotential, which is equivalent to the chemical potential of adsorbed hydrogen [23]. Therefore, η_2 is related to the hydrogen fugacity (f_{H_2}) through the Nernstian relationship in Eq. (6) [22,24,25]:

$$-f\eta_2 = \frac{1}{2} ln\left(\frac{f_{H_2}}{f_{H_{2,0}}}\right) \quad (6)$$

where $f=F/RT$, F is Faraday's constant, R is the gas constant, and T is temperature in K, and $f_{H_{2,0}}$ is the fugacity of hydrogen at standard state (here assumed to be 1 atm). Since the chemical potential of adsorbed hydrogen is equivalent to that of the absorbed hydrogen at steady state (i.e. the Penetration reaction is at equilibrium), Zhang et al. derived the following equation relating η_2 and x [25]:

$$-f\eta_2 = 6.44 - \frac{6031.13\ K}{T} + x\frac{5409.65\ K}{T} + ln\left(\frac{x}{1-x}\right) - 0.5ln(f_{H_{2,0}}) \quad (7)$$

This equation only applies for β-PdH_x when $x \geq 0.71$. One can then compare x obtained from the experiments to the equivalent f_{H_2} necessary to obtain that x from gas loading by using the

relationships in Eqs. (6) and (7). For example, a f_{H_2} of about 1420 atm is required to obtain x=0.86. Fig. 3(a) shows the equivalent f_{H_2} that would be required to obtain the η_2 from different currents and Pb amounts.

When η_2 is plotted vs log(|j|) it is possible to determine whether the predominant reaction route occurs via the Volmer-Tafel or the Volmer-Heyrovsky pathway by examining the shape of the curve [22,26,27]. Such studies have shown that a Volmer-Tafel reaction route results in a linear relationship. It is then customary to define the intercept of the linear fit of η_2 vs log(|j|) as the exchange current density of the Tafel reaction, enabling analysis of the Tafel reaction kinetics. On the other hand, if the reaction proceeds through the Volmer-Heyrovsky reaction route a potential plateau is observed as the cathodic current density is increased. Previous analysis of Pd cathodes performed in this way have mostly shown linear relationships in η_2 vs log(|j|) "Tafel plots," leading authors to suggest the dominant reaction route is the Volmer-Tafel route [22,26,27].

Fig. 3(a) shows a η_2 vs log(|j|) Tafel Plot and corresponding linear fits for selected experiments and Pb addition amounts. At low Pb amounts, the relationship is linear, indicating the Volmer-Tafel mechanism as the dominant reaction route. The Tafel plots remain fairly linear for Pb amounts up to 23 μg cm^{-2}, where a potential plateau near −0.1 V is clearly evident. Therefore, the trends observed in Fig. 3(a) suggest a transition of the primary reaction route from Volmer-Tafel to Volmer-Heyrovsky as the Pb amount is increased within the investigated current range.

Assuming the linear regions in the Tafel plots are indicative of a predominantly Volmer-Tafel reaction route, the intercepts (j_{o2}) of the linear fits could shed some light on the kinetics of the Tafel reaction. Since j_{o2} is representative of the exchange current density of the Tafel reaction, a smaller j_{o2} is indicative of a slower rate of the Tafel reaction. The resulting j_{o2} of the most linear regions obtained from the Tafel Plots are shown in Fig. 3(b) vs Pb amount. An interesting

observation from this plot, which also overlays the data from Fig. 1(d), is that there is an inverse relationship between j_{o2} and the maximum hydrogen content. Thus, analyzing the data this way indicates the Tafel rate is slowest when the highest x is observed at a Pb amount around 3 μg cm^{-2}. Slower Tafel kinetics is also often used to describe the mechanism for nonmetallic hydrogen insertion promoters [3,7,8].

The slope of η_2 vs log(|j|) can also be used to obtain information about the HER reaction route. The slope for the Pd samples in this work was −31±6 mV dec^{-1}, in agreement with the −33 mV dec^{-1} obtained in alkaline electrolytes by Enyo and Biswas [24]. The slopes of the linear fits then become steeper as more Pb was added, down to roughly −130 mV dec^{-1}, as shown in Fig. 3(c). It is interesting to note that other studies observed a steeper slope for samples that also showed potential plateaus in the η_2 vs log(|j|) analysis [28]. In addition, clean Pd cathodes have also shown potential plateaus at current densities above 100 mA cm^{-2} [24]. Therefore, it is believed that the slope is a result of the applied current density at which the potential plateau is observed, i.e. when the Heyrovsky reaction becomes dominant. Regrettably, the limitations of the experimental configuration prevented the study of larger current densities, so this remains speculation. Alternatively, fitting these data with kinetic models [29,30] for the Volmer, Heyrovsky, and Tafel reactions could also elucidate the relationships between the rates as a function of Pb amount, which is work currently underway.

Regardless, the current work suggests a delicate interplay between the rates of the reactions (Volmer, Tafel, and Heyrovsky) which controls the electrochemical hydrogen insertion. The

observation of the potential plateau and analysis of j_{o2} and the slope of η_2 vs log(|j|) plots suggests a transition in the predominant reaction route from Volmer-Tafel to Volmer-Heyrovsky within the investigated current range. In the middle of this transition, a "sweet-spot" is found where the amount of Pb near 3 μg cm^{-2} changes the reaction rates such that the maximum amount of hydrogen can be inserted into the Pd cathode. Therefore, this work provides evidence that surfaces can be engineered to achieve enhanced hydrogen insertion under given working conditions. It is anticipated that different surfaces will affect the reaction rates to different extents, so the assistance of *ab initio* modelling would be beneficial in this regard in the same way it is assisting the engineering of HER catalysts [31–33].

3.5. Absorption Kinetics.

To determine the absorption kinetics as a function of Pb amount, the x vs time data was fitted for the first 2000 s of each current step using the following exponential relationship:

$$x = x_i - b \cdot exp\left(-\frac{t}{\tau}\right) \qquad (8)$$

where t is the time elapsed since the change in applied current, x_i is the H/Pd ratio at the beginning of the step, b is the amplitude, and τ is the hydrogen insertion time constant. For the two largest applied currents, the 23 μg cm^{-2} Pb sample needed the addition of an extra exponential term with a time constant 2-3 orders of magnitude larger than the first time constant to obtain a good fit. Once again, fitting the data with kinetic models may be necessary to understand this second time constant, but will not be discussed in this work. Fig. 4 shows τ vs Pb amount at a selected current step of −9.0 mA cm^{-2} to −11 mA cm^{-2}. The relationship between τ and Pb amount appears to be exponential and shows that larger amounts of Pb results in a larger τ. This indicates the H insertion within Pb regions is much slower than Pd regions, and further addition of Pb blocks exposed Pd.

4. CONCLUSION

The enhancement of hydrogen insertion in palladium after the addition of lead to an alkaline electrolyte was experimentally demonstrated. By performing a sensitivity study on the amount of added Pb up to 23 μg cm^{-2}, an optimum amount of 2.9 μg cm^{-2} was found for the maximum insertion at an electrode potential of about −0.5 V vs RHE. The results suggest a change in the individual HER reaction rates, and that the insertion enhancement is a result of the Pb changing the Volmer, Tafel, and Heyrovsky reaction rates. Increasing the amount of Pb was found to decrease the rate of hydrogen insertion. Overall, the work is a first step in engineering surfaces to provide further enhancements in the maximum electrochemical hydrogen storage capability.

AUTHOR INFORMATION

Corresponding Author

*Corresponding author. Tel.: +1 720 565 9690.

E-mail address: steven@coolescence.com (S.C. Hamm)

ACKNOWLEDGMENTS

The authors would like to thank Ed Goulet for taking the ICP-MS measurements, and Dr. Ariel Jackson for taking the XPS and depth profiling measurements.

Appendix A. Supplementary data

Supplementary data associated with this article can be found, in the online version, at http://dx.doi.org/XXXX

REFERENCES

[1] P. Tripodi, D. Di Gioacchino, R. Borelli, J.D. Vinko, Possibility of high temperature superconducting phases in PdH, Phys. C Supercond. 388 (2003) 571–572. doi:10.1016/S0921-4534(02)02745-4.

[2] P. Zhou, W. Li, X. Zhu, Y. Li, X. Jin, J. Chen, Graphene Containing Composite Coatings as a Protective Coatings against Hydrogen Embrittlement in Quenching & Partitioning High Strength Steel, J. Electrochem. Soc. 163 (2016) D160–D166.

[3] J. Kafle, D. Qu, Enhancement of hydrogen insertion into carbon interlayers by surface catalytic poisoning, J. Phys. Chem. C. 114 (2010) 19108–19115. doi:10.1021/jp1064006.

[4] B. Fang, H. Zhou, I. Honma, Ordered porous carbon with tailored pore size for electrochemical hydrogen storage application, J. Phys. Chem. B. 110 (2006) 4875–4880.

[5] T. Zakroczymski, Z. Szklarska-śmiałowska, M. Śmiałowski, Effect of promoters on the permeation of electrolytic hydrogen through steel, Mater. Corros. 27 (1976) 625–630. doi:10.1002/maco.19760270904.

[6] G. Zheng, B.N. Popov, R.E. White, The Role of Thallium as a Hydrogen Entry Promoter on Cathodically Polarized HY-130 Steel, J. Electrochem. Soc. 141 (1994) 1526–1532. doi:10.1149/1.2054957.

[7] D. Liu, D. Zheng, L. Wang, D. Qu, Z. Xie, J. Lei, L. Guo, B. Deng, L. Xiao, D. Qu,

Enhancement of Electrochemical Hydrogen Insertion in N-Doped Highly Ordered Mesoporous Carbon, J. Phys. Chem. C. 118 (2014) 2370–2374. doi:10.3389/fenrg.2014.00042.

[8] L. Gao, B.E. Conway, Absorption and adsorption of H in the H2 evolution reaction and the effects of co-adsorbed poisons, Electrochim. Acta. 39 (1994) 1681–1693. doi:10.1016/0013-4686(94)85154-9.

[9] B.E. Conway, G. Jerkiewicz, Thermodynamic and electrode kinetic factors in cathodic hydrogen sorption into metals and its relationship to hydrogen adsorption and poisoning, J. Electroanal. Chem. 357 (1993) 47–66. doi:10.1016/0022-0728(93)80373-P.

[10] G. Jerkiewicz, P. Marcus, eds., Proceedings of the Symposium on Electrochemical Surface Science of Hydrogen Adsorption and Absorption, in: The Electrochemical Society, 1997: pp. 180–199.

[11] R.N. Iyer, I. Takeuchi, M. Zamanzadeh, H.W. Pickering, Hydrogen Sulfide Effect on Hydrogen Entry into Iron—A Mechanistic Study, Corrosion. 46 (1990) 460–468. doi:10.5006/1.3585133.

[12] F.A. Lewis, A. Aladjem, Hydrogen in Metal Systems II, Scitec Publications, 2000.

[13] W.S. Zhang, Z.F. Zhang, Z.L. Zhang, Some problems on the resistance method in the in situ measurement of hydrogen content in palladium electrode, J. Electroanal. Chem. 528 (2002) 1–17. doi:10.1016/S0022-0728(02)00845-8.

[14] R.J. Smith, D.A. Otterson, Electrical resistivity of PdHx system for H/Pd atom ratios to 0.97, J. Phys. Chem. Solids. 31 (1970) 187–189.

[15] D.L. Knies, V. Violante, K.S. Grabowski, J.Z. Hu, D.D. Dominguez, J.H. He, S.B. Qadri, G.K. Hubler, In-situ synchrotron energy-dispersive x-ray diffraction study of thin Pd foils with Pd : D and Pd : H concentrations up to 1 : 1, J. Appl. Phys. 112 (2012) 83510.

[16] M.P. Mercer, D. Plana, D.J. Fermín, D. Morgan, N. Vasiljevic, Growth of Epitaxial Pt1-x Pb x Alloys by Surface Limited Redox Replacement and Study of Their Adsorption Properties, Langmuir. 31 (2015) 10904–10912. doi:10.1021/acs.langmuir.5b02351.

[17] P. Quaino, F. Juarez, E. Santos, W. Schmickler, Volcano plots in hydrogen electrocatalysis - uses and abuses., Beilstein J. Nanotechnol. 5 (2014) 846–54. doi:10.3762/bjnano.5.96.

[18] T. Yoshida, T. Yamaguchi, Y. Iida, S. Nakayama, XPS Study of Pb(II) Adsorption on γ-Al 2 O 3 Surface at High pH Conditions, J. Nucl. Sci. Technol. 40 (2003) 672–678. doi:10.1080/18811248.2003.9715405.

[19] D. Chadwick, M.A. Karolewski, XPS and UPS study of Pb monolayers on polycrystalline Pd, Surf. Sci. 126 (1983) 41–48. doi:10.1016/0039-6028(83)90693-3.

[20] V.I. Nefedov, Y. V Salyn, P.M. Solozhenkin, G.Y. Pulatov, X-ray photoelectron study of surface compounds formed during flotation of minerals, Surf. Interface Anal. 2 (1980) 170–172.

[21] O.T. Holton, J.W. Stevenson, The Role of Platinum in Proton Exchange Membrane Fuel Cells, Platin. Met. Rev. 57 (2013) 259–271. doi:10.1595/147106713X671222.

[22] T. Maoka, M. Enyo, Overpotential Decay Transients and the Reaction Mechanism on the Pd–H2 Electrode, Surf. Technol. 8 (1979) 441–450.

[23] F.A. Lewis, Molecular Hydrogen Diffusion Overpotential and Local Cell Hydrogen

Transfer Processes at Electrodes of Palladium, Palladium Alloys and Other Transition Metals, and Implications for Theories of Hydrogen Overpotential, Surf. Technol. 11 (1980) 1–16.

[24] M. Enyo, P.C. Biswas, Hydrogen Absorption in Palladium Electrodes in Alkaline-Solutions, J. Electroanal. Chem. 335 (1992) 309–319. doi:Doi 10.1016/0022-0728(92)80250-8.

[25] W.-S. Zhang, X.-W. Zhang, H.-Q. Li, The maximum hydrogen (deuterium) loading ratio in the Pd|H2O (D2O) electrochemical system, J. Electroanal. Chem. 434 (1997) 31–36. doi:10.1016/S0022-0728(97)00043-0.

[26] T. Maoka, M. Enyo, Hydrogen absorption by palladium electrode polarized in sulfuric acid solution containing surface active substances—I. The cathodic region, Electrochem. Acta. 26 (1981) 607–614.

[27] T. Green, D. Britz, Kinetics of the deuterium and hydrogen evolution reactions at palladium in alkaline solution, J. Electroanal. Chem. 412 (1996) 59–66. doi:10.1016/0022-0728(96)04589-5.

[28] M. Elam, B. Conway, Sorption behavior of the overpotential-deposited H species in the cathodic H2 evolution reaction at Pd and Pt-Pd electrode composite electrodes, J. Electrochem Soc. 135 (1988) 1678–1685. doi:10.1149/1.2096096.

[29] S.A. Vilekar, I. Fishtik, R. Datta, Kinetics of the Hydrogen Electrode Reaction, J. Electrochem. Soc. 157 (2010) B1040–B1050. doi:10.1149/1.3385391.

[30] P.M. Quaino, M.R. Gennero de Chialvo, A.C. Chialvo, Hydrogen electrode reaction: A

complete kinetic description, Electrochim. Acta. 52 (2007) 7396–7403. doi:10.1016/j.electacta.2007.06.030.

[31] E. Skúlason, V. Tripkovic, M.E. Björketun, S. Gudmundsdóttir, G. Karlberg, J. Rossmeisl, T. Bligaard, H. Jónsson, J.K. Nørskov, Modeling the electrochemical hydrogen oxidation and evolution reactions on the basis of density functional theory calculations, J. Phys. Chem. C. 114 (2010) 18182–18197. doi:10.1021/jp1048887.

[32] J. Greeley, T.F. Jaramillo, J. Bonde, I.B. Chorkendorff, J.K. Nørskov, Computational high-throughput screening of electrocatalytic materials for hydrogen evolution., Nat. Mater. 5 (2006) 909–13. doi:10.1038/nmat1752.

[33] Q. Lu, G.S. Hutchings, W. Yu, Y. Zhou, R. V Forest, R. Tao, J. Rosen, B.T. Yonemoto, Z. Cao, H. Zheng, J.Q. Xiao, F. Jiao, J.G. Chen, Highly porous non-precious bimetallic electrocatalysts for efficient hydrogen evolution, Nat. Commun. 6 (2015). doi:10.1038/ncomms7567.

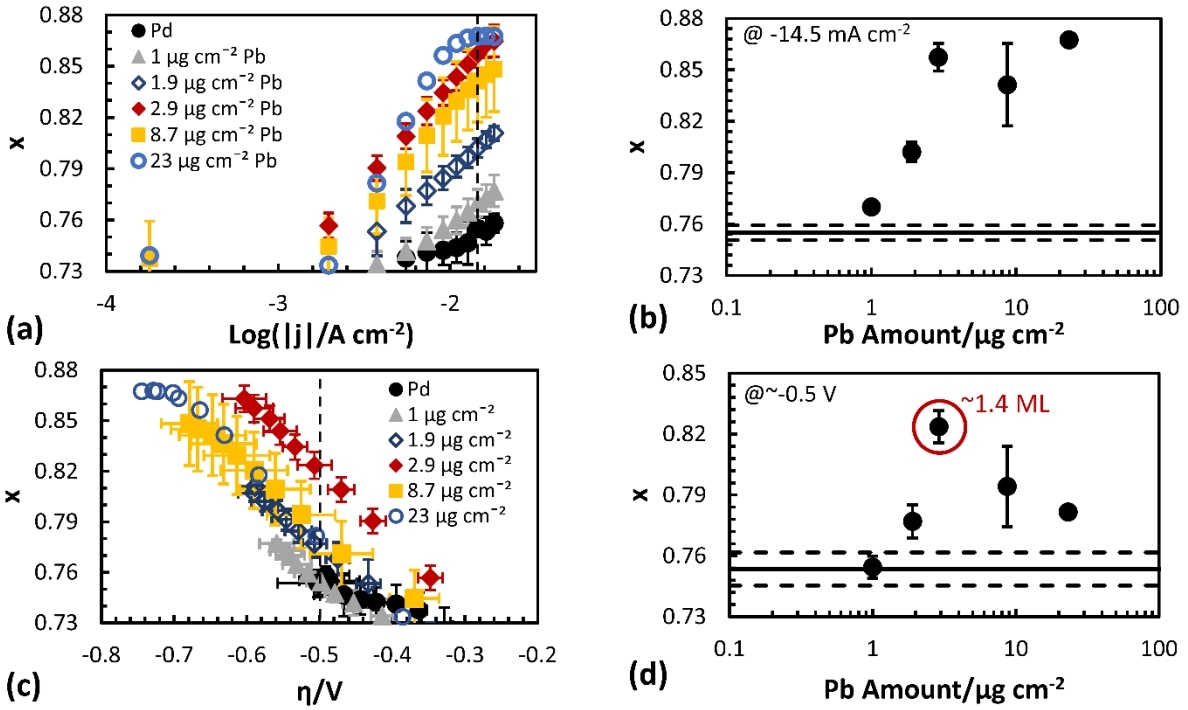

Fig. 1. (a) Hydrogen content, *x*=H/Pd, versus current density for the various Pb addition amounts, (b) *x* vs Pb amount at a constant current of −14.5 mA cm^{-2}, (c) *x* vs η measured at each applied current for various Pb addition amounts, and (d) *x* vs Pb amount obtained near the measured overpotential of −0.5 V. Vertical dashed lines in (a) and (c) indicate the conditions used to plot (b) and (d), respectively. The solid and dashed horizontal lines in (b) and (d) indicate the mean and one standard deviation for the control Pd obtained at that condition, respectively. These plots indicate the optimum amount of Pb is around 3 μg cm^{-2} (~1.4 mass equivalent ML).

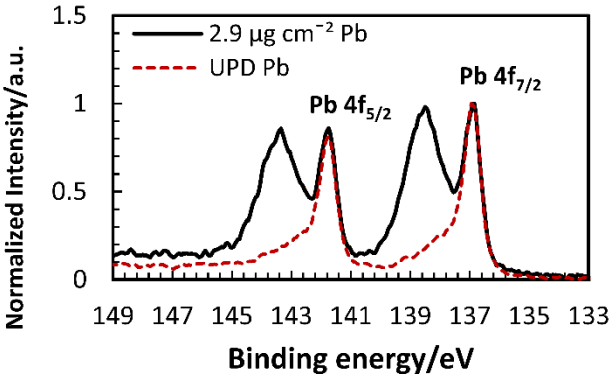

Fig. 2. Normalized Pb 4f X-ray photoelectron spectra for a sample with 2.9 µg cm^{-2} Pb added during electrolysis and a sample with Pb deposited by UPD. The peaks at 143.4 eV and 138.4 eV are indicative of $Pb(OH)_2$, which is believed to have formed after the experiment.

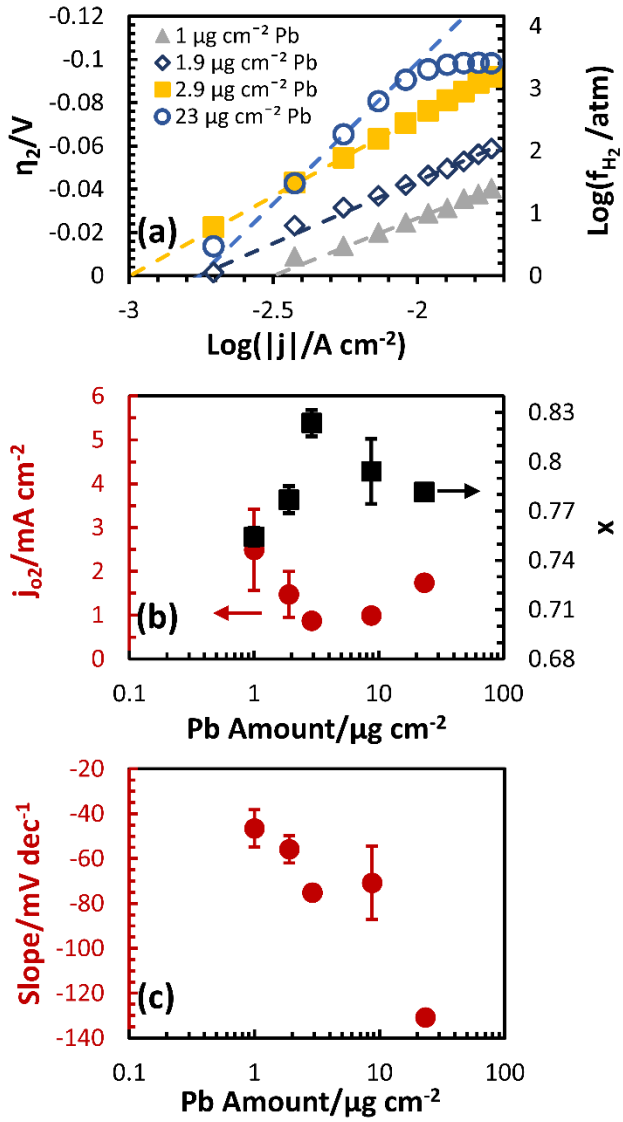

Fig. 3. (a) Hydrogen overpotential (η_2) "Tafel Plot" obtained from one iteration of the different Pb amounts. The equivalent hydrogen fugacity (f_{H_2}) that would be required to obtain the reported η_2 from gas loading is also shown for comparison. A linear "Tafel Plot" is representative of the Volmer-Tafel route, and the observation of a potential plateau in the "Tafel Plot" is representative of the Volmer-Heyrovsky route [22,26]. (b) j_{o2} vs Pb amount obtained from the intercept from the linear fits of the "Tafel Plots", and (c) the "Tafel Plot" slopes vs Pb amount. The hydrogen content, *x*, is replotted from Fig. 1(d). Error bars show one standard deviation for the three measurements.

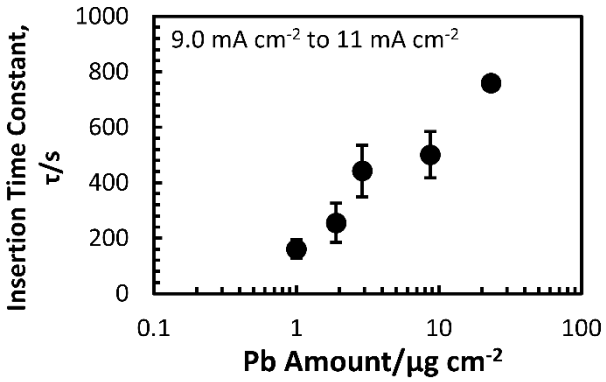

Fig. 4. Insertion time constant, τ vs Pb amount for the −9.0 mA cm^{-2} to −11 mA cm^{-2} step. More Pb increases the amount of time required to reach a steady-state hydrogen content.